Astron. Astrophys. 105, 98–106 (1982)

ASTRONOMY AND ASTROPHYSICS

"Flip-flop" of Electric Potential of Dust Grains in Space*

N. Meyer-Vernet

CNRS, LA 264, Departement de Recherches Spatiales, Observatoire de Meudon, F-92190 Meudon, France

Received June 16, accepted August 18, 1981

Summary. It is shown that, contrary to what is generally believed, the charge on a cosmic grain is not always unique: the equilibrium equation may have multiple roots, when the main charging mechanisms are particle fluxes from the ambient plasma and secondary emission. If the plasma is thermal, the grain's surface should have an exceptionally high secondary emission yield for multiple roots to occur; but if the plasma is non-thermal and not too cold, multi-valued potentials should occur frequently on non-metallic grains.

This phenomenon, which stems from the fact that there are two different values of the incident electron energy giving the same secondary yield and which is already known for spacecrafts, has some important consequences:

(i) identical grains in the same environment (but with different histories) may have opposite charges;

(ii) a small change in the environment may induce large and rapid charge's variation;

(iii) one may conjecture that in suitable conditions, the charge could oscillate.

Several consequences on the grain accretion, dynamics, and radio-emission are briefly outlined. The results may be relevant for the discharge-like radio-emission recently discovered by Voyager I near Saturn.

Key words: grains – interplanetary dust – interstellar matter physical processes – Saturn

I. Introduction

The charge on cosmic grains has been widely studied (see Spitzer, 1978; Feuerbacher et al., 1973; Mendis and Axford, 1974), owing to its effects on the physical and dymical processes in the interplanetary, interstellar and intergalactic media; most recently, Voyager spacecraft's results have emphasized its importance in the Saturnian rings environment (Warwick et al., 1981).

The basic problem is to solve the equilibrium equation $dQ/dt = I(\varphi) = 0$, where φ is the grain's potential, and the current I must take into account the relevant charging processes. The solution φ is generally believed (and in fact often found) to be unique.

However, when the ambient electrons are sufficiently energetic for secondary emission to be important, the solution may be multiple, owing to the bi-valued nature of the incident energy as a function of the secondary electron yield.

Such a possibility had been conjectured long ago by Whipple (1965), and spacecraft-charging specialists have found recently that the potential of a shaded surface in geosynchronous orbit may be multivalued, when the secondary electron emission yield is larger than one, and the plasma is not Maxwellian (Prokopenko and Laframboise, 1977, 1980).

Since similar conditions are likely to occur in several instances for cosmic grains, it is worth investigating the process. In Sect. II, we discuss the occurrence of multiple valued grain potentials. Some consequences on the physics of grains and cosmic bodies are outlined in Sect. III.

II. When Multiple Roots Occur

We do not intend to undertake a precise study of the most general case. Instead, we consider some simplified situations, where multiple roots occur, in order to emphasize the main physics of the problem. The problem is defined in Sect. II.1; Sect. II.2 considers a thermal plasma; Sect. II.3 a non-thermal plasma; the hypotheses and results are discussed in Sect. II.4.

1. Position of the Problem

We consider a spherical grain or small body immersed in a plasma of ions (H^+) and electrons, and assume that the main charging mechanism comes from the fluxes of these particles. It is well-known that, if suffcently energetic particles are present, secondary emission becomes important. Typically, the electron yield δ (i.e. the ratio of emitted electrons to incident ones) is a function of the primary electrons energy E, peaking at an energy $E_M \approx 300$–2000 eV. This maximum δ_M is of the order of unity for metals and semiconductors, and of order 2–30 for insulators (Bruining, 1954); it depends on the physical and chemical state of the surface.

The function $\delta(E)$ can be approximated by the widely used relation (Sternglass, 1954):

$$\delta(E) = 7.4\,\delta_M E/E_M \exp\left[-2(E/E_M)^{1/2}\right]. \quad (1)$$

(We neglect its variation with the incidence angle of primary electrons.)

The velocity distribution of emitted electrons can be approximated by a Maxwellian with thermal energy $E_s = kT_s \sim 1$–5 eV (Bruining, 1954). In addition, we neglect the secondary emission due to ion impact, and the reflection and backscattering of particles (see Sect. II.4).

* In honour of the 60th birthday of Andrei Dmitrevich Sakharov

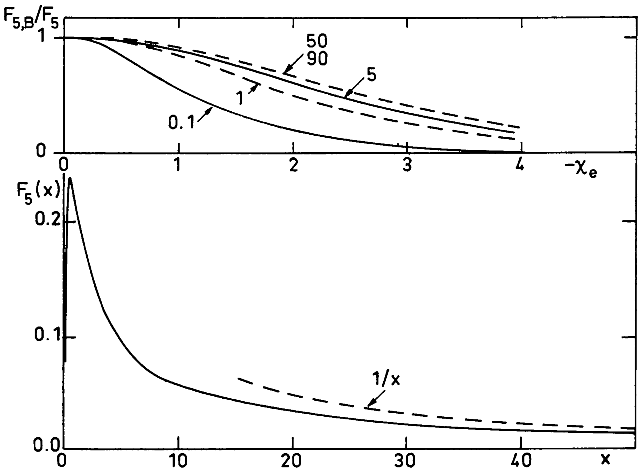

Fig. 1. Bottom part: Function $F_5(x)$; the function $1/x$ is plotted for comparison. Upper part: $F_{5,B}(x)/F_5(x)$ [where $B=(-\chi_e/x)^{1/2}$] is plotted as a function of $-\chi_e$ for different values of x

To define completely the problem, we need the distribution function of incident particles. We take a Maxwellian (temperature T_i) for the ions; for the electrons we take a Maxwellian in Sect. II.2, and a Maxwellian plus a supra-thermal Maxwellian or a power-law in Sect. II.3. This gives reasonably simple final expressions and keeps the numerical calculations to a minimum. Sanders and Inouye (1979) have studied the bi-Maxwellian case for a spacecraft in synchronous terrestrial orbit, by replacing Eq. (1) by an approximation of it; Prokopenko and Laframboise (1977, 1980) have studied numerically a spacecraft situation with a composite power-law spectrum.

Following them, we assume that the flux of incoming as well as escaping particles is orbital-motion limited, which represents rather general situations (Laframboise and Parker, 1973) and poses no problem at least for cosmic bodies smaller than the Debye-length. In this case, the incoming flux of electrons (e) or ions (i) has the form:

$$J_{e,i}=\int_{\max(0,\pm e\varphi)}^{\infty}(1\pm(-e\varphi/E))\,dj_{e,i}/dE\quad dE, \tag{2}$$

where φ is the grain's surface potential and the signs $-$, $+$ correspond to electrons and ions, respectively; $dj_{e,i}/dE=(2\pi E/m_{e,i}^2)\times dn_{e,i}/d^3v$ is the ambient energy-differential electron (ion) flux[1] incident on one side of an arbitrary oriented surface element; and $dn_{e,i}/d^3v$ is the ambient electron (ion) velocity distribution.

If $\varphi<0$, the secondary emitted electron flux is:

$$J_{\rm sec}=\int_{-e\varphi}^{\infty}(1+e\varphi/E)\,dj_e/dE\;\delta(E+e\varphi)\;dE. \tag{3}$$

On the other hand, if $\varphi>0$, not all the secondary electrons will escape, and one finds, following Prokopenko and Laframboise (1980):

$$J_{\rm sec}=(1-\chi_s)\exp(\chi_s)\int_0^{\infty}(1+e\varphi/E)\,dj_e/dE\;\delta(E+e\varphi)\;dE, \tag{4}$$

1 In the non-relativistic approximation

where

$\chi_s=-e\varphi/kT_s$.

2. Maxwellian Plasma

In this section, the ambient electron velocity distribution is assumed to be Maxwellian, thus:

$$dj_{e,i}/dE=(2\pi E/m_{e,i}^2)\,n_{e,i}(m_{e,i}/2\pi kT_{e,i})^{3/2}\exp(-E/kT_{e,i}) \tag{5}$$

then, Eq. (2) gives the well-known result:

$$J_{e,i}=J_{0e,i}\times\begin{cases}\exp(-\chi_{e,i}) & \text{if } \chi_{e,i}>0\\ 1-\chi_{e,i} & \text{if } \chi_{e,i}<0,\end{cases} \tag{6}$$

where

$\chi_{e,i}=\mp e\varphi/kT_{e,i}$

and

$J_{0e,i}=n_{e,i}(kT_{e,i}/2\pi m_{e,i})^{1/2}$,

and the signs $-$ $(+)$ correspond to electrons (ions). (i.e. $\chi_{e,i}$ is negative for attracted particles).

For the secondary electron flux, Eqs. (1) and (3) give in a straightforward way, for $\varphi<0$:

$$J_{\rm sec}=3.7\,\delta_M J_{0e}\exp(-\chi_e)F_5(E_M/4kT_e), \tag{7}$$

where:

$$F_5(x)=x^2\int_0^{\infty}u^5\exp-(xu^2+u)\,du.$$

The function $F_5(x)$ is easily calculated (Appendix 1) and is shown in Fig. 1.

For $\varphi>0$, Eqs. (1) and (4) yield:

$$J_{\rm sec}=3.7\,\delta_M J_{0e}(1-\chi_s)\exp(\chi_s-\chi_e)F_{5,B}(E_M/4kT_e) \tag{8}$$

where

$$F_{5,B}(x)=x^2\int_B^{\infty}u^5du\exp-(xu^2+u)\qquad\text{(see Fig. 1)}$$

and

$B=(-\chi_e/(E_M/4kT_e))^{1/2}$.

The potential is then obtained from the current balance equation:

$$J_T=J_i-(J_e-J_{\rm sec})=0. \tag{9}$$

Taking $n_e=n_i$ (ambient charge neutrality), the solution χ_e depends on four dimensionless parameters:

δ_M, E_M/kT_e, T_s/T_e, T_i/T_e.

Depending on the ambient plasma and the grain's surface properties, the range of parameters may be very large. However, in most cases, the following constraints are in order: $\delta<30$ (typically less); $E_M/kT_s\simeq 100$–2000 (from Sect. II.1), and $T_i/T_e\sim 1$.

For $\varphi<0$ ($\chi_e>0$) Eqs. (6)–(7) show that Eq. 9 has only one solution if: 1–$3.7\,\delta_M F_5(E_M/4kT_e)>(m_eT_i/m_iT_e)^{1/2}$; and no solution otherwise.

On the other hand, for $\varphi>0$, the discussion is not so easy and requires examining the functions $F_5(x)$ and $F_{5,B}(x)$ (Fig. 1). One sees that solutions may a-priori exist in the case $E_M/4kT_e\gg 1$, $T_s/T_e>1$ (note that if $T_s/T_e=1$ there is no solution), and 3.7 δ_M

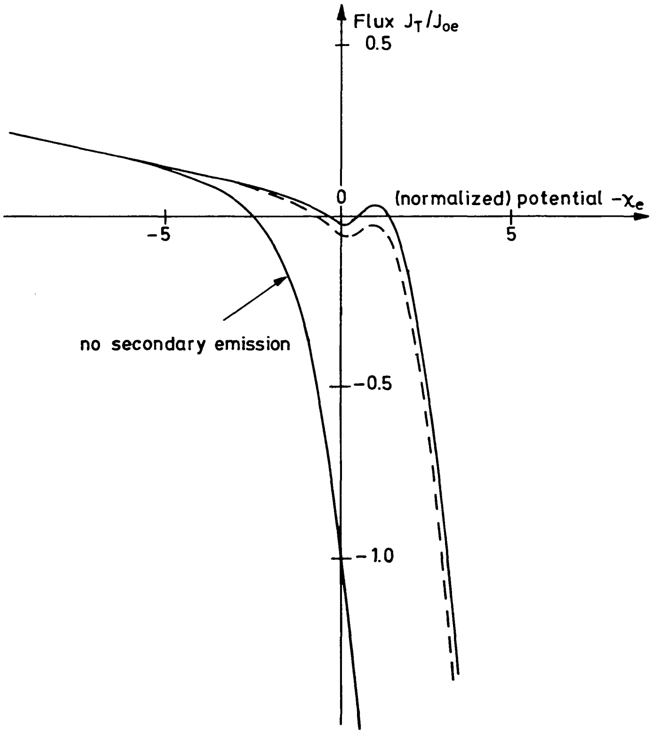

Fig. 2. Net flux of charge (normalized) J_T/J_{0e} as a function of the (normalized) surface's potential $-\chi_e = e\varphi/kT_e$, for parameters yielding two positive roots, or not. Maxwellian plasma, $T_i = T_e$; secondary emission parameters: $T_s/T_e = 1.5$, $\delta_M = 15$ and $E_M/4\,kT_e = 45.6$ (full line) and 47.0 (broken line). (Note that these secondary emission parameters are not typical, contrary to those in Figs. 7 and 8). A curve with no secondary emission is plotted for comparison

$\sim E_M/4kT_e$ [since $F_5(x) \sim x^{-1}$ for $x \gg 1$, and since $m_eT_i/m_iT_e \ll 1$].

Figure 2 shows the total current as a function of χ_e for one set of parameters chosen in this range and following the above constraints. In these cases, Eq. (9) has three roots.

Figure 3 shows the domain of parameters δ_M and E_M/kT_e (with $T_i/T_e = 1$ and $E_M/kT_s = 120$) where triple roots occur. We note that this corresponds to very high secondary yields and a comparatively low value of E_M/kT_s (this will be discussed in Sect. II.4). For higher values of E_M/kT_s, the domain where multiple roots occur, moves to higher values of δ_M.

Figure 4 shows how the roots change with the plasma temperature: near the cusps of the curve, an infinitesimal change in the plasma temperature changes a triple root situation into a single root one (or the opposite).

3. Non-Maxwellian Electrons

In planetary and interplanetary environments, suprathermal electrons are present. We shall approximate them by adding to the previous distribution [Eq. (5) where n_e becomes $n_e - n_H$]:

either (i) a hot Maxwellian (temperature $T_H > T_e$; density $n_H < n_e - n_H$ or (ii) a power law with index-2 in the high energy tail, namely (to avoid discontinuous functions):

$$dj_{0H}/dE = (2\pi E/m^2)A_H(E_H + E)^{-3}, \tag{10}$$

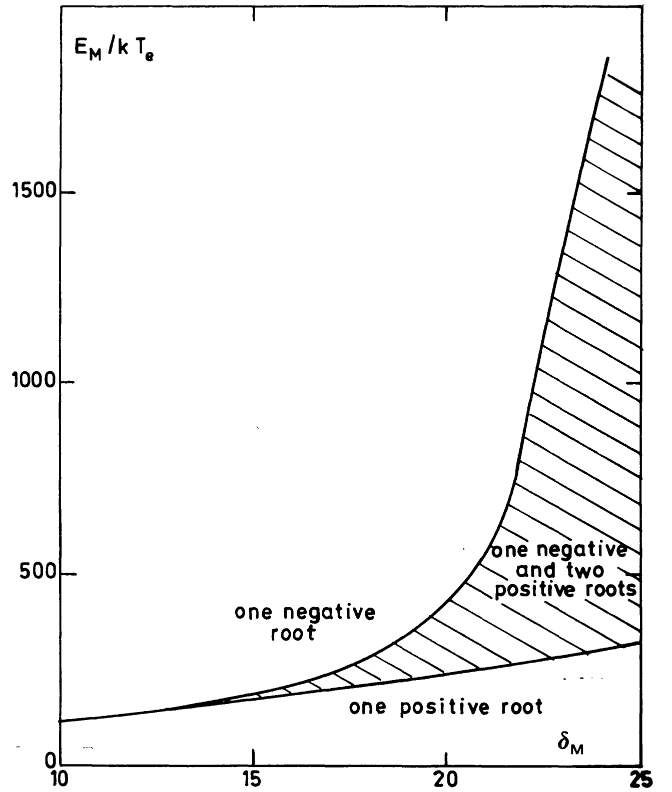

Fig. 3. Domain of parameters where a triple root situation occurs in a Maxwellian plasma (with $T_i = T_e$), for $E_M/kT_s = 120$

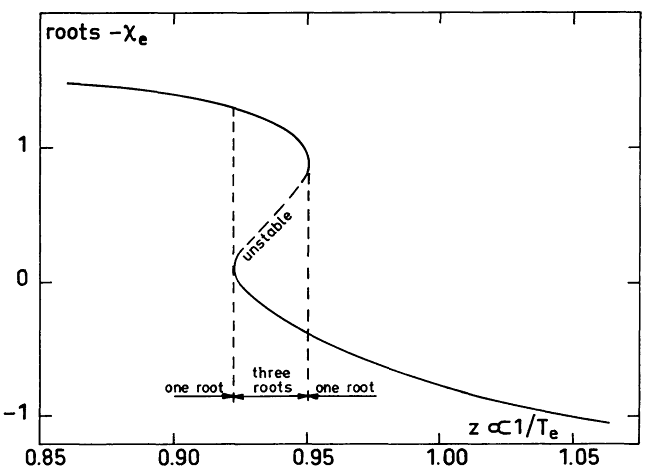

Fig. 4. Variation of the roots $-\chi_e$ as a function of the plasma temperature near a triple root situation (the parameter z represents the temperature as: $E_M/4\,kT_e = 48\,z$; $T_s/T_e = 1.5\,z$); $T_i = T_e$; $\delta_M = 15$

where the corresponding electron population has the density $n_H < n_e - n_H$ satisfying: $A_H = 2^{1/2}n_H\pi^{-2}(mE_H)^{3/2}$.

Both expressions represent a wide range of physical situations in different environments (see for example Feldman et al., 1975; Krimigis et al., 1981). Finally, we assume plasma neutrality, thus $n_i = n_e$.

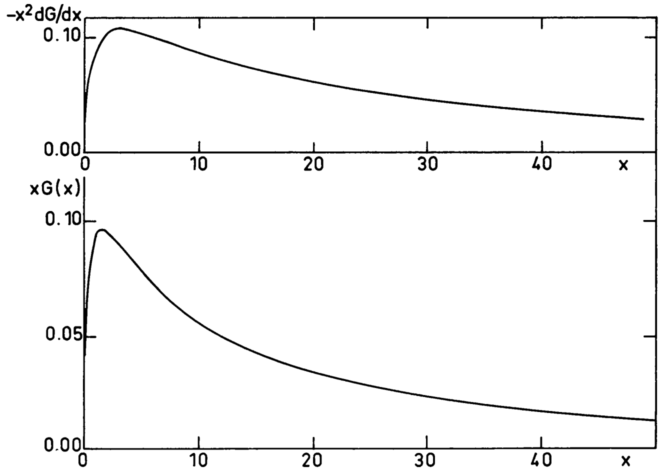

Fig. 5. Bottom part: plot of $xG(x)$, upper part: plot of $-x^2\,dG/dx$

Thus, in case (i), the incident electron flux (and the secondary flux) are obtained by adding to Eq. (6) [and to Eq. (8)] an identical term where n_e and T_e are to be replaced by $n_{\rm H}$ and $T_{\rm H}$ [while n_e becomes $n_e - n_{\rm H}$ in Eqs. (6) and (8)].

On the other hand, in case (ii), the incident hot electron flux is given by using Eqs. 2 and 10 as:

$$J_{e{\rm H}} = 2\pi A_{\rm H}/m^2 \int_{\max(0,-e\varphi)}^{\infty} (E+e\varphi)\,(E_{\rm H}+E)^{-3}\,dE$$
$$= 2J_{0e}(E_{\rm H}/\pi kT_e)^{1/2} n_{\rm H}/n_e \begin{cases} (1-e\varphi/E_{\rm H})^{-1} & \text{if} \quad \varphi<0 \\ (1+e\varphi/E_{\rm H}) & \text{if} \quad \varphi>0. \end{cases} \tag{11}$$

Likewise, the secondary electron flux due to the hot electrons is obtained in case (ii) by using Eqs. (3) or (4), and Eq. (10) as:

$$J_{\rm sec\,H} = (2\pi/m^2)\,7.4\,A_{\rm H}\delta_M/E_M \int_{\max(-e\varphi,0)}^{\infty} dE(E+e\varphi)^2$$
$$\cdot\,(E_{\rm H}+E)^{-3} \exp\left[-2((E+e\varphi)/E_M)^{1/2}\right] \times \begin{cases} 1 & \text{if } \varphi<0 \\ (1-\chi_s)\exp\chi_s & \text{if } \varphi>0 \end{cases}$$
$$= 8J_{0e}(n_{\rm H}/n_e)(E_{\rm H}/\pi kT_e)^{1/2}\,7.4\,\delta_M E_{\rm H}/E_M \times \begin{cases} G_0\left[4(E_{\rm H}-e\varphi)/E_M\right] & \text{if } \varphi<0 \\ G_B\left[4(E_{\rm H}-e\varphi)/E_M\right]\times(1-\chi_s)\exp(\chi_s) & \text{if } \varphi>0, \end{cases} \tag{12}$$

---

where $B=(4e\varphi/E_M)^{1/2}$ as in Sect. II.2, and the function $G_B(x)$ is defined as:

$$G_B(x) = \int_B^{\infty} u^5(u^2+x)^{-3}\exp(-u)\,du.$$

The function G is easily calculated (Appendix 1) and shown in Fig. 5.

The current balance equation is now:

$$J_T = J_i - (J_e - J_{\rm sec}) - (J_{e{\rm H}} - J_{\rm sec\,H}) = 0. \tag{13}$$

First, we note that:

$$J_T/J_{0e} \sim \chi_e (m_e T_e/m_i T_i)^{1/2} > 0 \quad \text{for} \quad \varphi \to -\infty$$

$$J_T/J_{0e} \sim \chi_e [1 - n_{\rm H}/n_e + n_{\rm H}/n_e \times \begin{cases} (T_e/T_{\rm H})^{1/2}] & \text{(i)} \\ 2(kT_e/\pi E_{\rm H})^{1/2}] & \text{(ii)} \end{cases} \quad \text{for} \quad \varphi \to +\infty$$
$$< 0.$$

Thus, (as in Sect. II.2) the number of roots is odd (except if the curve J_T is tangent to the axis).

Now, at variance with the previous section, it is possible to find two roots in the range $\varphi<0$.

For the bi-Maxwellian plasma [case (i)], the balance equation for $\varphi<0$ has the form:

$$a\exp(-\chi_e) + a_{\rm H}\exp(-\chi_e T_e/T_{\rm H}) = b(1+\chi_e T_i/T_e),$$

where:

$$a = (1-n_{\rm H}/n_e)\,[1-3.7\,\delta_M F(E_M/4kT_e)]$$

$$a_{\rm H} = n_{\rm H}/n_e[1-3.7\,\delta_M F(E_M/4kT_{\rm H})]\,(T_{\rm H}/T_e)^{1/2}$$

$$b = (m_i T_i/m_e T_e)^{1/2}.$$

The derivative of the left-hand term is zero for a normalized potential $\chi_e=\chi_0$ given by:

$$\chi_0(1-T_e/T_{\rm H}) = {\rm Ln}\,(-aT_{\rm H}/a_{\rm H}T_e)$$

and the condition for two roots in the range $\varphi<0$ ($\chi_e>0$) is: $a<0$; $0<a_{\rm H}<\min\,(|a|+b,\ |a|\,T_{\rm H})$; $a(1-T_{\rm H}/T_e)\exp(-\chi_0)>b\,(1+\chi_0 T_e/T_i)$. In particular, (see Fig. 1), it is necessary that:

$$3.7\,\delta_M > {\rm Max}\,(1/0.24,\ E_M/4kT_e); \qquad E_M/4kT_{\rm H} < 0.5.$$

Figure 6a shows, as an example, the range of values of $n_{\rm H}/n_e$ and $T_{\rm H}/T_e$ where two negative roots occur for the parameters $\delta_M=3$; $E_M=400$ eV; $T_s=2$ eV (which are typical values for SiO_2) and $T_e=25$ eV, $T_i/T_e=1$.

A typical curve $I(\varphi)$ corresponding to these values is shown in Fig. 7.

Now, let us examine the power-law case (ii). The balance equation for $\varphi<0$ has the form:

$$a\exp(-\chi_e) + a_{\rm H}[1-7.4\,\delta_M y G(y)]/y = b(1+\chi_e T_i/T_e)$$

where:

$$a_{\rm H} = 2\pi^{-1/2} n_{\rm H}/n_e (E_{\rm H}/kT_e)^{3/2}/(E_M/4kT_e)$$

$$y = \frac{\chi_e + E_{\rm H}/kT_e}{E_M/4kT_e} \qquad \text{(and } a,\ b \text{ as defined above).}$$

The derivative of the left-hand term is:

$$-a\exp(-\chi_e) - a_{\rm H}(1+7.4\,\delta_M y^2 dG/dy)/y^2.$$

In particular, one sees immediately that it is always negative (see the function $y^2 dG/dy$ in Fig. 5) and there are no multiple roots for $\varphi<0$ if $3.7\,\delta_M<\min\,(E_M/4kT_e,\ 1/(2\times 0.108))$.

In the general case, the conditions, which involve the parameters δ_M, E_M/kT_e, $E_{\rm H}/kT_e$, T_i/T_e, $n_{\rm H}/n_e$, are rather cumbersome.

Figure 6b shows the range of values of $n_{\rm H}/n_e$ and $E_{\rm H}/kT_e$ where two negative roots occur for the same parameters as in Fig. 6a.

A typical curve $I(\varphi)$ corresponding to these values is shown in Fig. 7.

Figure 8 shows, with the same parameters, how the roots change with the proportion $n_{\rm H}/n_e$ of suprathermal particles.

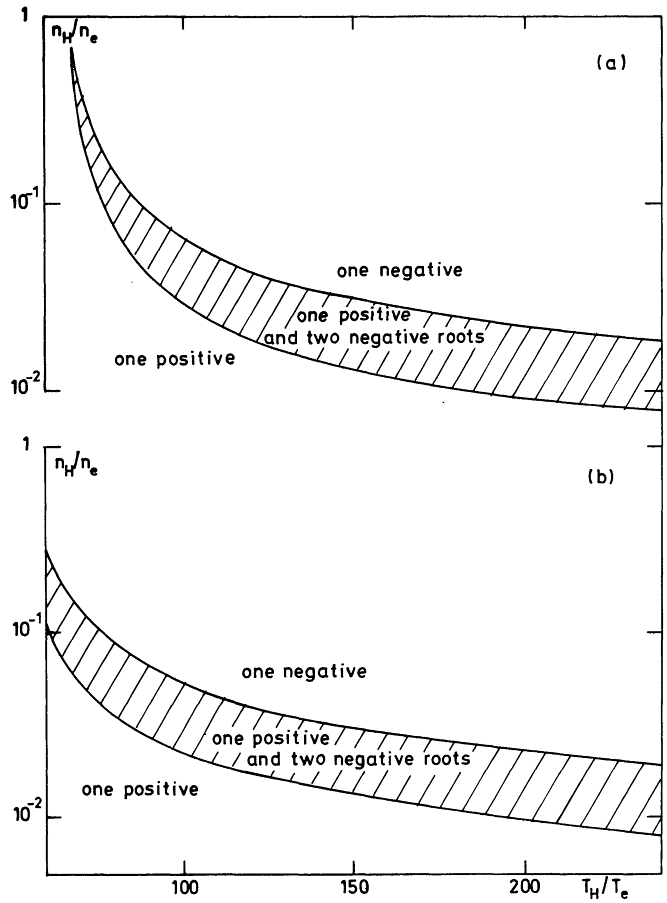

Fig. 6a and b. Range of suprathermal electrons (normalized) density n_H/n_e and energy $T_H/T_e(a)$ or $E_H/kT_e(b)$ where a triple root situation occurs (hatched area) in the following case: cold plasma temperature $T_e = T_i = 25$ eV; secondary emission parameters typical for SiO_2: $\delta_M = 3$, $E_M = 400$ eV, $T_s = 2$ eV. **a** bi-Maxwellian electron distribution. **b** Cold Maxwellian plus a hot electrons distribution akin to a -2 power-law [Eq. (10)]

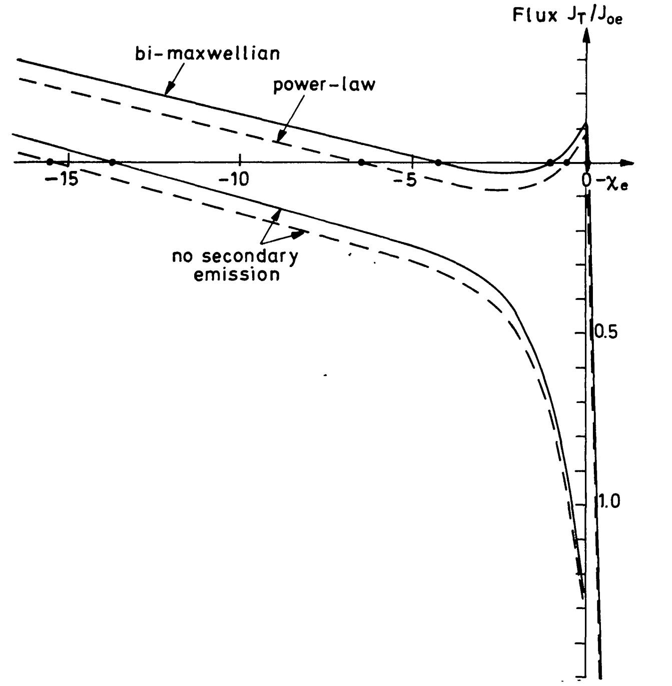

Fig. 7. Net flux of charge (normalized) J_T/J_{0e} as a function of the (normalized) potential $-\chi_e = e\varphi/kT_e$ for the same parameters as Fig. 6 in the cases: bi-Maxwellian: $n_H/n_e = 0.04$, $T_H/T_e = 100$ (full line), Maxwellian plus power-law: $n_H/n_e = 0.04$, $E_H/kT_e = 100$ (broken line). The case with no secondary emission is shown for comparison

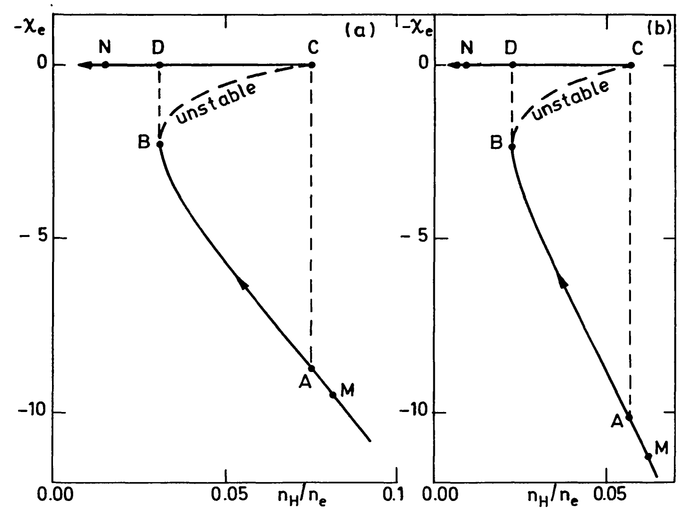

Fig. 8 a and b. Variation of the roots $-\chi_e = e\varphi/kT_e$ with the relative density n_H/n_e of suprathermal electrons. The other parameters are the same as in Figs. 6 and 7; **a** bi-Maxwellian: $T_H/T_e = 100$. **b** Maxwellian plus power-law: $E_H/kT_e = 100$. When the density decreases from M (or increases from N) the potential jumps from B to D (or from C to A)

4. Discussion

In order to display the main physics of the multiple-root situation and obtain simple expressions, we have neglected several charging processes. In particular, we have neglected photoemission, velocity anisotropy, secondary emission due to ion impact, and reflection and backscattering of particles.

Neglecting *photoemission* means that the grain should either be sufficiently far from a hot star (or shadowed) or in a sufficiently dense plasma, or have a very low photoemission yield. Broadly speaking, the photoelectron saturation flux J_{ph} should be negligible[2] with respect to the ambient electron flux, of order (at zero potential) J_{0e}. This condition is generally satisfied in H_I regions for low yield photoemitters, and in H II regions for most photoemitters (Feuerbacher et al., 1973). Concerning the solar system environment, let us consider the two extreme cases of a high photoemitter (Aluminium oxide) and a low photoemitter (graphite) at distance $R_{A.U.}$ from the Sun. Using data from Grard (1972) one finds: $4J_{ph} \sim 0.25 \leftrightarrow 2.6 (10^{14}/R^2_{A.U.})$ electrons s^{-1} m^{-2}; (the factor 4 stems from the projection area).

Thus photoemission is expected to be negligible if the (Maxwellian) electrons density and temperature satisfy the inequality:

2 In Fig. 7, for instance, a photoelectron flux of order 0.1 J_{0e} is sufficient to make the multiple root disappear

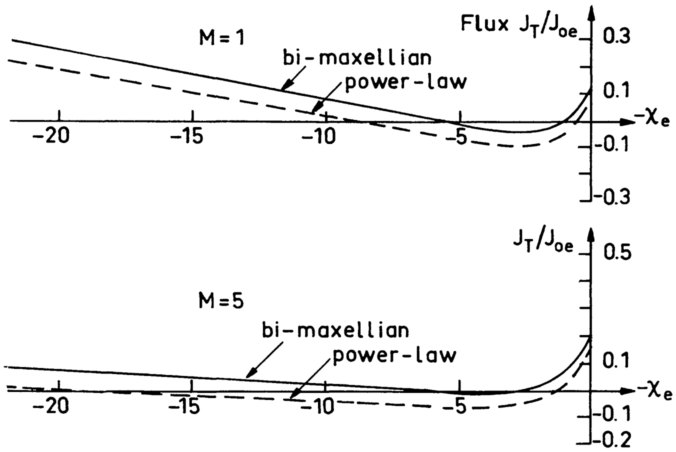

Fig. 9. Same as Fig. 7 but there is a plasma-to-grain mean velocity V such that: $M=(m_i V^2/2kT_i)^{1/2}=1$ (top) and 5 (bottom)

Table 1. Secondary emission data

Material	δ_M	E_M (eV)
Fe	1.3	350
C (graphite)	1	250
SiO_2 (quartz)	2.1–4	400
Mica	2.4	350
Al_2O_3	2–9	350–1300
CaO	2.2	500
MgO	3–25	400–1500

$$n_{e(\mathrm{cm}^{-3})}(T_e/10^5\ \mathrm{K})^{1/2}R^2_{\mathrm{A.U.}} \gg 10 \leftrightarrow 100$$

which is realized in planetary ionospheres, in Jupiter's inner magnetosphere, and in some plasma environments of the equatorial planes of Jupiter (Warwick et al., 1979) and Saturn (Bridge et al., 1981), and also possibly outside the orbit of Saturn.

Concerning the *anisotropy* of the ambient distribution function due to the grain-to-plasma relative velocity, we note that this velocity is generally low with respect to the electron thermal velocity; thus, in general, only the ion flux (if any) is appreciably modified. If the potential is negative (and the grain small with respect to the Debye length) the ion flux in Eq. 6 is to be replaced by the well-known expression (see Whipple, 1965):

$$J_i = J_{0i}[\pi^{1/2} erF(M)\ (0.5+M^2+|\chi_i|)/M + \exp\ (-M^2)]/2, \qquad (14)$$

where $M=(m_i V^2/2kT_i)^{1/2}$ and V is the grain-to-plasma relative velocity.

The domain of multiple roots situations is modified accordingly. As an example, Fig. 9 shows the flux J_T when $M=1$ (which is a typical value when V corresponds to planetary co-rotation speeds), and the other parameters as in Fig. 7. One sees that, in this case, the anisotropy does not change very much the results. For comparison, we have also plotted the case $M=5$, which is relevant for solar wind parameters. It yields also a multiple root situation; for higher velocities, the multiple root disappears in the bi-Maxwellian plasma case.

Neglecting electrons *backscattering* is probably not justified for incident electron energies much higher than about 5 keV (Kazan and Knoll, 1968). Moreover, taking account of it should restrict the domains of parameters where multiple roots occur (Prokopenko and Laframboise, 1980). We merely neglect it because of the scarcity of data[3] for materials relevant for grains. In addition in actual environment, the existence of *suprathermal ions* is not always negligible. The secondary emission due to ion impact is important for ions energies above several KeV. Thus, the present results become dubious for incident energies of electrons or ions larger than several KeV.

Finally, we note that our *description* of the secondary emission itself is uncertain, since it is based on laboratory data, which could be irrelevant for cosmic grains. Indeed, the high dependence of the yield on the physical and chemical structure of the surface is well-known; furthermore, laboratory measurements have been carried out for surfaces temperatures of order 300–1000 K which is much higher than the actual grains temperature in most cases, and it is known that $\delta \propto T^{-1/2}$ for insulators with few lattice defects. On the other hand, if the grain is smaller than the mean depth of production of secondary electrons ($\sim 10^{-2}$ μ), the yield is modified. Likewise, one should take into account the yield increase with increasing the angle of incidence of primary electrons. On the other hand, if the grain is in the form of an aggregate with a rough surface, the yield is lowered (Bruining, 1954).

Keeping these restrictions in mind, and in the absence of data for icy surfaces, we recall in Table 1 some published results (see Bruining, 1954; Whetten, 1962) which may be relevant for grains and cosmic solid bodies.

Viewing these data, the occurrence of three roots in a Maxwellian plasma (Sect. II.2) is expected to be rare since it necessitates both a high yield and a relatively low value of E_M/kT_s.

On the other hand, the secondary emission parameters used in Sect. II.3 seem rather realistic for non-metallic surfaces; furthermore, several earth-alkaline oxides have still larger values of δ_M, and exhibit multiple roots in plasmas nearer to the equilibrium. Thus, multiple roots could occur frequently, provided there is a few per cent of supra-thermal electrons, whether they have a Maxwellian or power-law velocity distribution. Typically, the thermal population temperature should be higher than a few 10 eV, and the suprathermal higher than several 100 eV.

These values are rather typical in the solar wind; they may also occur in planetary magnetospheres, including the Jovian (Warwick et al., 1979) and Saturnian (Krimigis et al., 1981) environments. Besides, it is not unlikely that they could exist in hot H_{II} regions, Seyfert nuclei, supernovae remnants and the intergalactic medium (in the latter cases, the temperature may be too hot for the present description to be valid; see Burke and Silk, 1974).

III. Consequences

Thus, multivalued potentials can exist on cosmic grains. The possible consequences depend on the stability of the roots. In the cases studied in Sects. II.2 and II.3, we found three roots. The middle root is unstable (see Prokopenko and Laframboise, 1977, 1980), since a negative (or positive) shift in the potential increases (or decreases) the negatively charging current. In this vicinity, the plasma-to-grain electric resistance is negative. On the other hand, the extreme roots are stable, and of opposite sign.

3 In fact, it is not possible to separate exactly the backscattered (rediffused) electrons from the "true" secondary ones since their energy distributions overlap slightly

This has important consequences on the grain physics, which are underlined below.

1. Grain Physics

(i) A grain in a given environment, will carry a charge corresponding to one of the stable equilibrium potentials. Thus *two identical* grains, *in the same environment*, but which have undertook different charging histories, *may have potentials of opposite sign* (as found for spacecrafts by the above authors).

(ii) When the grain's environment changes slowly with respect to the grain's charging time, the roots change as indicated for instance in Figs. 4 and 8. Suppose that the parameters are those corresponding to Fig. 8a, and that the density of suprathermal particles decreases from a value corresponding to point M.

The potential moves from M to A, B, and then *jumps*[4] to D, since the part B C is unstable. On the other hand, a density increase should result in a jumping from C to A. This mechanism has been suggested to explain large differential potentials on satellites in terrestrial orbits (see Besse, 1981). The potentials $\varphi_{A,B,C,D}$ are indicated in Table 2.

As an example, let us consider the cases of a grain of radius $a=1$ µ, and a 1 m solid body; the former grain's size is close to the threshold where the potentials found should cause electrostatic disruption (for most relevant material tensile strengths) and/or field emission (see Hill and Mendis, 1980). The corresponding charge Q (in electron charge units e) is indicated in Table 2[5].

Since the time-lag for secondary emission is negligible ($\tau_s < 3\ 10^{-11}$ s, Bruining, 1954), the typical grains charging time with these parameters is, broadly speaking:

$$\tau \gtrsim Q/(4\pi a^2 e J_{0e}) \sim \varepsilon_0 \varphi/(a e J_{0e}).$$

With the parameters as in Fig. 8, this yields, for the jump B–D:

τ (seconds) $\gtrsim 3\ 10^3/n_e$ (cm^{-3} for $a=1$ µ

τ (seconds) $\gtrsim 3\ 10^{-3}/n_e$ (cm^{-3}) for $a=1$ m

This gives the maximum changing rate of the grain's environment for this calculation of the charge's variation to be relevant; this yields also the typical duration of the jumps of charge.

(iii) Finally, we note that the region where the plasma-to-grain resistance is negative, is akin to the so-called dynatron characteristics well-known in vacuum tubes, which has been proposed to serve in building an *oscillator* tube (see Bruining, 1954). Likewise, one could imagine a mechanism in order to build an oscillatory system: for example, consider two adjacent portions 1, 2 of a (insulator) solid body, on different parts of the Curve 8a corresponding to charges of opposite sign; a change in the parameters triggers a jump of part 1 (say); if this jump modifies the parameters for part 2 in the opposite sense, on oscillating system is built. This could constitute an unexpected radioemitter if $1/\tau$ is in the radio-frequency range. However, owing to the complexity of the corresponding calculation, such a process is very speculative.

2. Practical Consequences

The present results are relevant for *grains accretion* and planetesimal formation. When the grain's separation is not very much larger than the Debye sheath, Coulombian forces between grains are important[6]. Grains of opposite charge attract each other electrostatically and eventually stick together. Since the resulting grain charge is not zero, this accretion process continues, until other mechanisms be dominant. This process has been suggested to occur between grains of different composition, when the photo-emission conditions ensure that these are oppositely charged (Feuerbacher et al., 1973). The present results show that, when secondary emission is important, this accretion process can occur between identical grains.

It is worth noting that, contrary to the process involving induced electrostatic charges (which can yield an attraction even between particles with charges of the same sign, if their sizes are very different), the above process works whether the particles have similar sizes or not and works not only at verry short range.

Another possible application concerns the *dynamics of grains in magnetic fields*. In recent calculations (Hill and Mendis, 1979, 1980) of the trapping of charged dust in outerplanetary magnetospheres, the (negative) sign of the grains charge plays an essential role: in Jupiter or Saturn case, where the spin and magnetic moments are approximately in the same sense, the Lorentz force tends to confine the negatively charged particles near the equatorial plane, and near the corotation distance. This is not the case for positively charged particles for which the electromagnetic force is in the opposite direction. In this context, the possible existence of identical grains with charges of both signs is relevant.

Finally, the present results, which should be applicable in the shadowed part (at least) of Saturn rings, are relevant in the discharge phenomenon recently suggested (Warwick et al., 1981) for explaining the sporadic *arc-like radio-emission* discovered by Voyager I.

A discharge requires the presense of a strong electrostatic field. The present results show that differentiated charging of identical grains or bodies, or between different parts of an insulating body could occur in Saturn rings. The latter case yields arc breakdowns inside the body, as occurs in spacecrafts.

Alternatively, the jumps of charge discussed in Sect. II.1, triggered by small environmental variations, play a similar role: in spherically symmetric conditions, a jump of charge emits plasma waves; but in practice, the process will be asymmetric and emit also electromagnetic waves; (the jump could also trigger charge's oscillations on the grain's surface). As a (rough) order of magnitude estimation, we take, for the energy involved (using the potentials in Table 2):

$W \sim 4\pi\varepsilon_0 a \varphi^2 \sim 10^{-5}\ a$ (SI units), for one particle of radius a. The observations (ibid.) show that an event involves at least 10^5 Joules. With the above value of W, this requires (for instance) $10^{10} \times a^{-1}$ bodies of radius a. Taking a filling factor of 10^{-2} (as currently assumed in the rings) and $a \sim 1$ m, gives a source size of $\sqrt[3]{10^{12}} = 10^4$ m, consistent with the experimental value (ibid.).

4 As stated below, the jump is in fact continuous. The curves of φ as a function of both parameters n_H/n_e and T_H/T_e (Figs. 6 and 8) suggest two-dimensional cross-sections of the popular "cusp-catastrophe" surface, which occurs in many different contexts (see, however, Zahler and Sussmann, 1977)

5 If the grain is small with respect to the Debye length, the sheath's capacitance is negligible and the charge on a spherical grain of radius a is $Q \simeq 4\pi\varepsilon_0 a \varphi$

6 The Coulombian interaction between grains dominates the gravitational one if the grain charge-to-mass ratio satisfies: $(Q/M)^2 > 4\pi\varepsilon_0 G$, i.e. (for grains with density 1) $a < 0.03\ \varphi^{1/2}$ (SI units); this interaction in turn results in accretion if the typical grain-to-grain relative velocity (V) and distance (d) satisfy (broadly speaking): $MV^2/2 \lesssim Q^2/4\pi\varepsilon_0 d$, thus $(ad)^{1/2} V < 2\ 10^{-7}\ \varphi$ (SI units)

Table 2. Potentials corresponding to Fig. 8, and associated charges on a grain of 1 μ radius

	A	*B*	*C*	*D*
Potential φ(V)	−218	−58	+0.25	+1.5
Charge Q/e if $a=1$ μ	$-1.5\ 10^5$	$-4\ 10^4$	$+1.7\ 10^2$	$+10^3$

A precise calculation of all these effects is outside the scope of the present paper; moreover, these are conjectural in view of our present poor knowledge of the relevant parameters.

IV. Conclusion

As was previously found for spacecrafts (Prokopenko and Laframboise, 1977, 1980), but contrary to a recent (insufficient) proof of unicity (Lafon et al., 1981), the charge equilibrium equation giving the potential on a cosmic grain can have multiple roots, if the main charging processes are particles fluxes from the ambient plasma, and secondary emission on the grain surface.

If the plasma is Maxwellian, multiple roots should occur in exceptional situations since they require secondary emission parameters rather rare according to the existing data. In this case, one finds one negative root and two positive ones. This possibility was overlooked in the papers on spacecraft charging, presumably because of its mostly academic relevance.

On the other hand, if the plasma is not Maxwellian (the suprathermal electrons being described by a hot Maxwellian or a power law), multiple roots should occur frequently if the electron secondary yield is greater than one (which is the rule for insulating materials) and the main electron population is hotter than several 10 eV, and there is a few percent electrons hotter than several 100 eV. In this case, one finds two negative roots and one positive one. Two of the roots are stable, and, for instance, a quartz particle in a slightly non-thermal 10 eV plasma has stable equilibrium potential values of −200 and +1 V.

The corresponding bifurcation phenomena have important consequences on the physics of cosmic grains and solid bodies and/or small planetary setellites devoid of atmosphere:

– two grains (or parts of a body), with the same composition and geometry in the same environment can have charges of opposite sign;

– a small variation in the parameters may cause an important jump of potential and charge;

– more conjecturally, in suitable conditions, a charge oscillation could occur.

These processes are relevant for the grains accretion and dynamics, and for explaining discharge-like phenomena in Saturn rings.

Acknowledgements. I thank Dr. A. Boischot [of the Voyager (PRA) scientific team] who kindly made me aware of relevant preprints and information.

Appendix 1

Function $F_5(x)$

Define: $F_n(x)=x^2 \int_0^\infty u^n \exp-(xu^2+u)\,du.$

Integrating by parts yield the recurrence formula:

$2xF_{n+1}(x)+F_n(x)=nF_{n-1}(x) \quad \text{for} \quad n \geqq 1, \quad x>0.$

F_0 is given by (Abramowitz and Segun, 1968, p. 302):

$F_0(x)=x^2(\pi/x)^{1/2} \exp\,(1/4x)\,[1-erF(1/2x^{1/2})]/2.$

Integrating by parts yields:

$F_1(x)=[x^2-F_0(x)]/2x.$

Then $F_5(x)$ is easily calculated.

The following expansions are obtained:

$$x\to\infty \quad F_5(x)\sim\left(1-\frac{7}{16}\left(\frac{\pi}{x}\right)^{1/2}+\dots\right)\Big/x$$

$$x\to 0 \qquad F_5(x)\sim 5!x^2+\dots.$$

Function $G(x)$

Define: $G_{q,p}(x)=\int_0^\infty \frac{v^q}{(v^2+x)^p} \exp\,(-v)\,dv.$

Integrating by parts yields:

$$G_{q,p}(x)=\frac{1}{2(p-1)}\,[-G_{q-1,p-1}+(q-1)G_{q-2,p-1}] \quad \text{if} \quad p,q\geqq 2.$$

One uses (Abramowitz and Segun, 1968, p. 232):

$G_{01}=[ci(x^{1/2})\sin(x^{1/2})-si(x^{1/2})\cos(x^{1/2})]/x^{1/2}$

$G_{11}=-ci(x^{1/2})\cos(x^{1/2})-si(x^{1/2})\sin(x^{1/2}).$

Then $G(x)=G_{5,3}(x)$ is easily calculated.

The following expansions are obtained:

$$x\to\infty \quad G(x)\sim\frac{5!}{x^3}\dots$$

$$x\to 0 \quad G(x)\sim -0.75-0.577-0.5\,\mathrm{Ln}\,x.$$

References

Abramowitz, M., Segun, I.A.: 1968, Handbook of mathematical functions, Dover
Besse, A.L.: 1981, *J. Geophys. Res.* **86**, 2443
Bridge, H.S., et al.: 1981, *Science* **212**, 217
Bruining, H.: 1954, Physics and applications of secondary electron emission, Pergamon Press, London
Burke, J.R., Silk, J.: 1974, *Astrophys. J.* **190**, 1
Feldman, W.C., Ashbridge, J.R., Bame, S.J., Montgomery, H.D., Gary, S.P.: 1975, *J. Geophys. Res.* **80**, 4181
Feuerbacher, B., Willis, R.F., Fitton, B.: 1973, *Astrophys. J.* **181**, 101
Grard, R.J.L.: 1972, Properties of the satellite photoelectron sheath derived from photoemission laboratory measurements, Rep. ESTEC No. 663, ESRO
Hill, J.R., Mendis, D.A.: 1979, *The moon and the planets* **21**, 3
Hill, J.R., Mendis, D.A.: 1980, *The moon and the planets* **23**, 53

Kazan, B., Knoll, M.: 1968, Electronic image storage, Academic Press
Krimigis, S.M. et al.: 1981, *Science* **212**, 225
Lafon, J.P., Lamy, P.L., Millet, J.: 1981, *Astron. Astrophys.* **95**, 295
Laframboise, J.G., Parker, L.W.: 1973, *Phys. Fluids* **16**, 629
Mendis, D.A., Axford, W.I.: 1974, *Ann. Rev. Earth and Planetary Sci.* **2**, 419
Prokopenko, S.M.L., Laframboise, J.G.: 1977, in Rep. AFGL.TR. 77-0051, Air Force Geophys. Lab., Hanscom Air Force Base, Mass.
Prokopenko, S.M.L., Laframboise, J.G.: 1980, *J. Geophys. Res.* **85**, 4125
Sanders, N.L., Inouye, G.T.: 1979, in Rep. AFGL-TR-79-0082, Air Force Geophys. Lab., Hanscom Air Force Base, Mass.
Spitzer, L., Jr.: 1978, Physical processes in the interstellar medium, Wiley, Interscience
Sternglass, E.J.: 1954, Sci. Pap. 1772, Westinghouse Res. Lab., Pittsburgh, Pa.
Warwick, J.W. et al.: 1979, *Science* **204**, 995
Warwick, J.W. et al.: 1981, *Science* **212**, 239
Whetten, N.R.: 1962, Methods of experimental physics, Vol. IV, Academic Press, London
Whipple Jr., E.C.: 1965, The equilibrium electric potential of a body in the upper atmosphere and in interplanetary space, Ph. D. Thesis, Rep. X-615-65-296, Goddard Space Flight Center, Greenbelt, Maryland
Zahler, R.S., Sussmann, H.J.: 1977, *Nature* **269**, 759